Alignment dependent chemisorption of vibrationally excited CH4(3) on Ni(100), Ni(110), and Ni(111)

Bruce L. Yoder, Régis Bisson, P. Morten Hundt, and Rainer D. Beck

Related Articles

Interlayer molecular diffusion and thermodynamic equilibrium in organic heterostructures on a metal electrode
J. Appl. Phys. 110, 113709 (2011)

Influence of quantum effects on the physisorption of molecular hydrogen in model carbon foams
J. Chem. Phys. 135, 214701 (2011)

Constructing a new closure theory based on the third-order Ornstein-Zernike equation and a study of the adsorption of simple fluids
J. Chem. Phys. 135, 204706 (2011)

Kinetic and relativistic effects on the surface alloy formation of submonolayer Au adsorbed on Si(111)-×-Pb surface
Appl. Phys. Lett. 99, 211912 (2011)

Kinetics of gas mediated electron beam induced etching
Appl. Phys. Lett. 99, 213103 (2011)

Additional information on J. Chem. Phys.

Journal Homepage: http://jcp.aip.org/

Journal Information: http://jcp.aip.org/about/about_the_journal

Top downloads: http://jcp.aip.org/features/most_downloaded

Information for Authors: http://jcp.aip.org/authors

Alignment dependent chemisorption of vibrationally excited CH$_4$(ν_3) on Ni(100), Ni(110), and Ni(111)

Bruce L. Yoder,[1] Régis Bisson,[2] P. Morten Hundt,[3] and Rainer D. Beck[3,a)]

[1]*Department of Chemistry, University of British Columbia, 2036 Main Mall, Vancouver, British Columbia V6T 1Z1, Canada*
[2]*Aix-Marseille Univ, PIIM, CNRS, UMR 6633, 13397 Marseille, France*
[3]*Laboratoire de Chimie Physique Moléculaire, Ecole Polytechnique Fédérale de Lausanne, 1015 Lausanne, Switzerland*

We present a stereodynamics study of the dissociative chemisorption of vibrationally excited methane on the (100), (110), and (111) planes of a nickel single crystal surface. Using linearly polarized infrared excitation of the antisymmetric C–H stretch normal mode vibration (ν_3), we aligned the angular momentum and C–H stretch amplitude of CH$_4$(ν_3) in the laboratory frame and measured the alignment dependence of state-resolved reactivity of CH$_4$ for the $\nu_3 = 1$, J = 0–3 quantum states over a range of incident translational energies. For all three surfaces studied, in-plane alignment of the C–H stretch results in the highest dissociation probability and alignment along the surface normal in the lowest reactivity. The largest alignment contrast between the maximum and minimum reactivity is observed for Ni(110), which has its surface atoms arranged in close-packed rows separated by one layer deep troughs. For Ni(110), we also probed for alignment effects relative to the direction of the Ni rows. In-plane C–H stretch alignment perpendicular to the surface rows results in higher reactivity than parallel to the surface rows. The alignment effects on Ni(110) and Ni(100) are independent of incident translational energy between 10 and 50 kJ/mol. Quantum state-resolved reaction probabilities are reported for CH$_4$(ν_3) on Ni(110) for translational energies between 10 and 50 kJ/mol. © *2011 American Institute of Physics*. [doi:10.1063/1.3665136]

INTRODUCTION

Reactive collisions of gas phase molecules with solid surfaces are fundamental to many processes, both in nature and industry. The dissociative chemisorption of alkanes on transition metal catalysts is of specific importance in reforming processes for the production of fuels and several industrial chemicals.

Partly due to its rate limiting role in steam reforming for the production of hydrogen and/or synthesis gas, the dissociation of methane on nickel has become a prototype system for state-resolved studies of polyatomic gas/surface reaction dynamics. Early experiments using molecular beams with thermally prepared vibrations showed that methane dissociation is activated by both translational[1] and vibrational[2] energy. Then, the advent of laser-excited molecular beams permitted quantum state-resolved measurements which proved methane chemisorption to be both mode-specific[3] and bond-selective.[4] A recent review by Juurlink *et al.*[5] provides a thorough summary of the field.

Highly detailed state-resolved measurements provide stringent tests for the development of accurate theoretical models of gas/surface reactivity. Ultimately, the goal of gas/surface dynamics research is to develop a predictive understanding of reactivity at the gas/surface interface including heterogeneous catalysis. Early theoretical models of methane

dissociation were constrained to typically 3 or 4 dimensions believed to be the most important for the description of the microscopic dynamics of the reaction.[6–9] Lately, both experimental[10] and theoretical studies[11–13] highlighted the importance of considering additional degrees of freedom in order to understand CH$_4$ dissociation dynamics on transition metals. The most recent models[13, 14] are based on a 15 dimensional potential energy surface but still restrict the dynamics of the methane/surface to follow the lowest-energy reaction path i.e., the molecule is forced to reorient along its minimum energy configuration during its approach to the surface.

In a recent publication,[15] we reported a stereodynamics study of methane chemisorption on Ni(100) which seems contradictory to the assumption of gas molecules following their lowest energy pathway to reaction. Using a quantum state-prepared, laser aligned molecular beam of methane (CH$_4$(ν_3) and CD$_3$H(ν_1)), control was exerted over most aspects of the reactive encounter, including the approach direction and velocity, quantum state and relative alignment of the reaction partners. A 60% increase in CH$_4$(ν_3) reactivity was observed if methane's C–H stretch amplitude was aligned in the plane of the surface as compared to an alignment along the surface normal which resulted in the lowest reactivity. While there is not yet a definite explanation for the observed alignment dependence in methane dissociation, the observation that the methane reactivity depends on its initial vibrational alignment implies the absence of significant steering of the incident molecule along the lowest-energy reaction path on the sub-picosecond time scale of the reactive collision. Further

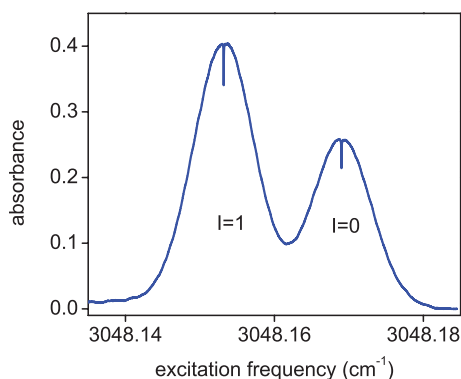a)Author to whom correspondence should be addressed. Electronic mail: rainer.beck@epfl.ch.

FIG. 1. Doppler broadened absorption lines of the (ν_3)-R(2) transitions of CH_4 with Doppler-free Lamb-dip features obtained with 70 mW of IR power in a 3 mm diameter laser beam retro-reflected through a 160 cm long room temperature absorption cell filled with 2 Pa of CH_4. For excitation of CH4 in the molecular beam, the OPO frequency was stabilized to a given rovibrational transition by locking to the Lamb-dip.

experiments described below show that a similar or even more pronounced steric effect occurs in the dissociation of $CH_4(\nu_3)$ on other crystallographic orientations of Ni as well as on Pt(111) which will prove helpful in clarifying the origin of the observed steric effects.

EXPERIMENTAL

The molecular-beam/surface science apparatus used for our quantum state-resolved reaction probability measurements has been described in detail previously[16] and only a brief summary of the experimental technique is given here. We prepare a continuous molecular beam of methane in a specific quantum state ($\nu_3 = 1$, J = 0, 1, 2, or 3) by resonant rovibrational excitation with continuous wave infrared radiation generated by an optical parametric oscillator (OPO, Argos model 2400, Lockheed Martin Aculight Corp.). In the work reported here, we performed rovibrational excitation with linearly polarized radiation in a single pass across the molecular beam, which selectively populates only a subset of the available M-levels for each J, creating an alignment of the angular momentum $\vec{J}$ and the C–H stretch amplitude of the rovibrationally excited methane molecules.[17,18] We stabilize the OPO idler frequency by first derivative locking to a Doppler-free saturation hole (Lamb-dip) in the center of the inhomogenously broadened Doppler profile (280 MHz FWHM, see Fig. 1) of the rovibrational transition of interest. The Lamb-dip is detected by splitting off a small fraction of the OPO idler output and retro-reflection through a 1.6 m absorption cell filled with 1–3 Pa of CH_4 at 300 K. By locking to the Lamb-dip of <1.5 MHz FWHM, the idler frequency could be kept in resonance with any of the rovibrational transitions of methane in the molecular beam during the 1–75 min deposition time.

Optical pumping of the molecular beam was achieved with up to 1 W of the OPO idler output focused by a f = +250 mm cylindrical lens to intersect the 2 mm diameter molecular beam at a right angle in a 1.4 × 3 mm ($1/e^2$ width) excitation region located 1 mm from the surface (see Fig 2). In contrast to previous state-resolved studies,[5] we per-
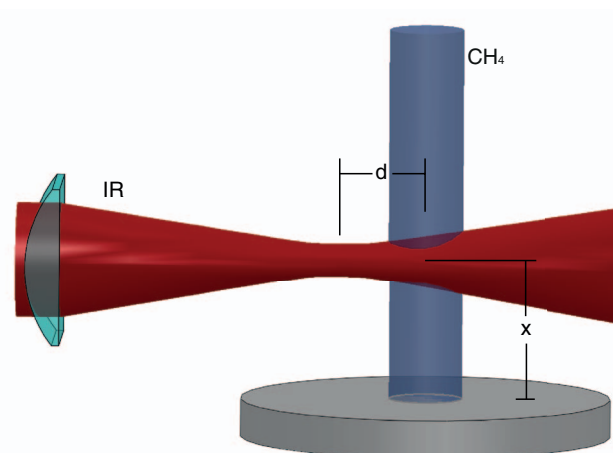

FIG. 2. Schematic of the geometry used for rovibrational state preparation of the incident methane by rapid adiabatic passage (not to scale). A seeded molecular beam containing CH_4 impinges at normal incident on a single crystal surface of nickel. At x = 1 mm from the surface, a continuous single mode infrared laser beam crosses the molecular beam at 90°. The IR beam is focused by a cylindrical lens (f = 250 mm) in the direction of the molecular beam to a waist located a distance d from the center of the molecular beam.

formed the laser excitation of the molecular beam in close proximity to target surface in order to minimize the loss of alignment by nuclear hyperfine depolarization.[19] The focal length and position of the cylindrical lens were chosen to create an IR radiation field with suitably curved wavefronts to achieve Doppler tuning through a rovibrational transition for the methane molecules as they move through the focused laser beam. This Doppler tuning in combination with a suitably strong excitation field leads to excitation via rapid adiabatic passage (RAP),[20] which allows for complete population inversion of the rovibrational transition used for excitation. Following a delay of 0.35–1 μs, depending on the molecular beam speed, the state-prepared, aligned methane molecules collide at normal incidence with a Ni single crystal, cleaned before each deposition experiment by Ar ion (1 keV) sputtering and high temperature annealing.

For the state-resolved methane reactivity measurements, we expose the clean Ni single crystal surface to a molecular beam of CH_4 either with or without laser excitation. While the nascent products of the dissociative chemisorption of CH_4 are CH_3(ads) and H(ads), the hydrogen quickly leaves the Ni surface by dehydrogenation of CH_3(ads) and recombinative desorption of H_2 at the surface temperature of 473 K, leaving only surface bound carbon atoms. We quantify the resulting carbon (C) coverage on the Ni surface by recording C and Ni signals by Auger electron spectroscopy at about 50 points across the surface (step size = 130 μm) in a computer controlled scan.[3,16] We calculate the average methane reactivity S_0(laser-on) and S_0(laser-off) with and without laser excitation from the detected carbon coverage divided by the incident methane dose which is monitored during the deposition by a calibrated mass spectrometer. The state-resolved reactivity $S_0(\nu_3 = 1, J)$ can be obtained from the average reactivities according to

$$S_0(\nu_3) = \frac{S_0(laser-on) - S_0(laser-off)}{f_{exc}} - S_0(v=0),$$

$$\tag{1}$$

FIG. 3. Angular distributions $P_J(\theta)$ for different values of the angular momentum alignment coefficients $A_0^{(2)} = 2, -1,$ and 0.

where $f_{exc.}$ is the fraction of the methane molecules in the beam prepared by the laser excitation in the rovibrationally excited state ($\nu_3 = 1$, J) and $S_0(v = 0)$ is the reactivity of methane in the vibrational ground state.

ROTATIONAL AND VIBRATIONAL ALIGNMENT BY OPTICAL PUMPING

Rovibrational excitation by linearly polarized light creates an alignment (i.e., an anisotropic population of |M| levels in the vibrationally excited state) of the rotational angular momentum $\vec{J}$ as well as the C–H stretch amplitude of the vibrationally excited methane $CH_4(\nu_3 = 1$, J) with respect to the polarization axis of the excitation laser due to the $\Delta M = 0$ selection rule. For example, excitation via an R(0) transition ($\Delta J = +1$ selection rule) transfers population from the initial $J'' = 0$, $M'' = 0$ level to the J = 1 final state. For linearly polarized excitation, only the M = 0 sublevel of the J = 1 final state is accessible, creating an alignment of $\vec{J}$ perpendicular to the polarization axis. The degree of alignment produced by excitation via a particular rovibrational transition can be quantified by rotational and vibrational alignment coefficients $A_0^{(2)}$ and β_{axis} which can take values between –1 and +2 or 0 and +2, respectively, depending on the transition used for optical excitation.[21]

For an aligned ensemble of molecules characterized by a value of $A_0^{(2)}$, the probability of finding $\vec{J}$ at an angle θ from the polarization axis is given by (Fig. 3):

$$P_J(\theta) = \frac{1 + \frac{1}{2} \cdot A_0^{(2)}(3\cos^2\theta - 1)}{4\pi}. \quad (2)$$

Zare and co-workers[22, 23] have calculated $A_0^{(2)}$ coefficients for excitation via P, Q, and R branch transitions in the limit of weak pumping, which assumes negligible changes in the populations of the initial M-levels produced by the laser pumping. In this case, the calculation of $A_0^{(2)}$ is simply the summation of the transition probabilities (square of the Clebsch-Gordan coefficients) between the initial and final M-levels, connected by the optical selection rules (here, $\Delta M = 0$ and for Q-branch transitions $M \neq 0$). With increasing initial J-value, the alignment produced by optical pumping is increasingly due to the M-dependence of the transition probability. However, for the transitions R(0), Q(1), and P(1) which all involve transitions from a single |M| level, the assumption of weak pumping is not required because the summation of Clebsch-Gordan coefficients reduces to a single term (i.e., a single allowed transition). Therefore, the $A_0^{(2)}$ coefficients for these three

transitions are the same for RAP excitation, which produces complete population transfer from the initial state. In other words, the alignment produced for P(1), Q(1), and R(0) excitation is simply a result of the $\Delta M = 0$ selection rule which remains valid under strong pumping conditions. The calculation of the $A_0^{(2)}$ coefficients for R(1) and R(2) excitation are easily modified assuming complete transfer for any allowed transition between M sublevels independent of the transition strength.

Angular momentum alignment defines the distribution of the molecules' rotational axis in the laboratory frame, which also creates a (rotationally averaged) alignment of molecular bonds and the vibrational amplitudes, i.e., the vibrational wavefunction in space if the molecule is in a vibrationally excited state. In the simplest case of a diatom, such as CO or a parallel vibration of a linear molecule, the stretched bond and the vibrational amplitude are parallel to each other and perpendicular to $\vec{J}$. The bond alignment resulting from linearly polarized vibrational excitation of linear molecules as well as for a parallel vibration for symmetric top molecules has been calculated by Zare[17,22] and can be described in terms of a vibrational alignment coefficient β_{axis}. The probability distribution of finding the net vibrational amplitude at an angle θ from the polarization axis is given by Eq. (2) where $A_0^{(2)}$ is replaced by β_{axis}. Note however, that in contrast to $A_0^{(2)}$, β_{axis} can take only positive values, indicating that the vibrational alignment is always parallel to the laser polarization axis for a parallel vibration. Here $CH_4(\nu_3)$ has been treated as a symmetric top with unresolved K-structure, as the K-levels of a given J-state are degenerate in a spherical top. The "figure axis" of $CH_4(\nu_3)$ has been considered as the axis containing the net vibrational C–H stretch amplitude.

In order to probe for an alignment dependence in the methane reactivity, we use a $\lambda/2$ waveplate to rotate the linear polarization axis of the excitation laser and measure
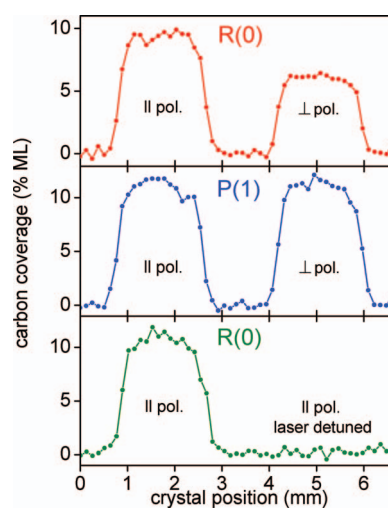

FIG. 4. Auger electron spectroscopy profiles detecting carbon coverage resulting from exposure of a clean Ni(100) surface to molecular beam (E_t = 34 kJ/mol) of $CH_4(\nu_3)$ excited 1 mm from surface with the excitation polarization parallel (left) and normal (right) to the surface plane. (Upper panel) Excitation via R(0) transition – strong alignment. (Middle panel) Excitation via P(1) – no alignment. (Lower panel) left- excited via R(0), right- laser slightly detuned from R(0) – no vibrational excitation.

S_0(laser-on) for polarization parallel ($S_0^\parallel$) and normal ($S_0^\perp$) to the plane of the surface. Figure 4 shows the Auger data resulting from such measurements for excitation via the R(0) and P(1) transition. The top panel shows the amount of carbon products detected after a pair of 15 min molecular beam exposures of $CH_4(\nu_3)$ prepared via the R(0) transition, with laser polarization rotated by 90° between the two exposures. We observe about 60% more carbon on the Ni(100) surface when polarization axis is parallel to the plane of the surface indicating a reactivity $S_0^\parallel$ that is ~60% higher than $S_0^\perp$.

To ensure that the observed reactivity changes between deposition experiments are due only to changes in the laser polarization axis, we perform identical measurements using excitation via the P(1) transition ($\Delta J = -1$) which does not create any alignment of $\vec{J}$ or the C–H stretch amplitude due to the fact that the excited state (v = 1, J = 0) consists of a single M = 0 sublevel. For P(1) excitation identical amounts of carbon products are detected for parallel and normal laser polarization excluding any potential experimental artifacts such as polarization dependent transmission of optical elements or variation in the overlap with the molecular beam due to rotation of the waveplate. Finally, to verify that all of the detected carbon is due to chemisorption of the laser prepared $CH_4(\nu_3 = 1, J)$, we repeated the deposition with the excitation laser on but detuned from resonance. In this case, no carbon deposition due to the impinging molecular beam is detectable, confirming that the reactivity of CH_4(v = 0) and any vibrationally excited methane due to heating in the expansion nozzle (T_n = 323 K) can be neglected.

ALIGNMENT CONTRAST Δ_p

From the observed polarization angle dependence, we quantify the alignment effect by defining an alignment contrast Δ_p:

$$\Delta_p(\nu_3, J) = \frac{S_0^\parallel(\nu_3, J) - S_0^\perp(\nu_3, J)}{S_0^\parallel(\nu_3, J) + S_0^\perp(\nu_3, J)}, \qquad (3)$$

where $S_0^\parallel(\nu_3, J)$ and $S_0^\perp(\nu_3, J)$ refer to the state-resolved reactivity measured with laser polarization parallel and normal to the plane of the surface, respectively. All Δ_p values were determined from at least 5 repeated measurements with the deposition coordinates for $\parallel$- and $\perp$-polarization alternated in order to cancel any potential local variations in surface reactivity of the nickel single crystal. We deposit up to four molecular beam spots with footprints of 2 mm ø on the 10 mm diameter Ni single crystal held at a surface temperature of 473 K.

In all experiments described here, the state-prepared, aligned molecular beam impinged at normal incidence on a nickel sample cut to within 0.1° of its (100), (110), or (111) plane. For the close-packed Ni(111) and Ni(100) samples, the azimuthal orientation of the surface relative to the $\parallel$- polarization axis (in-plane) was random and no attempt was made to check if the methane reactivity depended on this orientation. For the Ni(110) surface, which consists of close-packed rows of Ni atoms separated by one layer deep parallel troughs, we measured the reactivity with in-plane laser polarization either
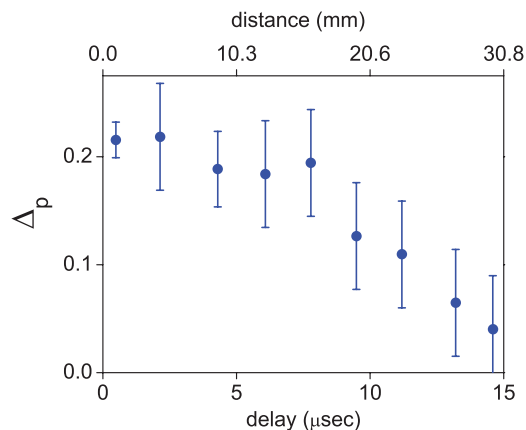

FIG. 5. Alignment contrast Δ_p for $CH_4(\nu_3)$ dissociation on Ni(100) for excitation via R(0) at different distances from the surface demonstrating the reduction in alignment with increasing time delay between excitation and surface impact due to hyperfine depolarization.

parallel or perpendicular to the close-packed rows. For these measurements, the close-packed rows of Ni(110) surface were aligned either parallel or perpendicular to the vertically polarized excitation laser by rotating the Ni(110) crystal in its sample mount. Low energy electron diffraction was used to verify the azimuthal alignment of close-packed rows on Ni(110) in the laboratory frame. We therefore distinguish the alignment contrast $\Delta_p(\varphi = 0°)$ and $\Delta_p(\varphi = 90°)$ for Ni(110), where the in-plane polarization axis is either parallel or perpendicular to the close-packed rows, respectively. Due to the cylindrical symmetry of $P_J(\theta)$ (Eq. (2)), the reactivity for normal polarization $S_0^\perp$ (ν_3, J) is independent of the azimuthal orientation.

HYPERFINE DEPOLARIZATION EFFECTS

The homogeneous linewidth of the CH_4 rovibrational transitions in the molecular beam are determined by transit time broadening to be 2–4 MHz for molecular beam speeds of 1000–2500 m/sec, significantly larger than the 50–90 kHz hyperfine splittings of CH_4.[24] Therefore, all hyperfine components of a given CH_4 rovibrational transition are excited coherently when CH_4 in the molecular beam passes through the laser beam. The optical excitation aligns the rotational angular momentum $\vec{J}$ but not the nuclear spin $\vec{I}$, which remains randomly oriented. Coupling between $\vec{J}$ and $\vec{I}$ to the conserved total angular momentum $\vec{F}$ will cause a dephasing (quantum beats) of the $\vec{J}$ alignment on the timescale of the inverse of the hyperfine splittings.[25] We observe this dephasing by measuring Δ_p for different excitation-to-surface distances over a range of 1–30 mm (Fig. 5). For a molecular beam speed of ~2000 m/sec (E_{TRANS} = 34 kJ/mol), this corresponds to a range of delays between $CH_4(\nu_3)$ excitation and surface collision of 0.5–15 μsec. A decrease of Δ_p from 0.22 ± 0.02 to 0.04 ± 0.05 is observed on this timescale, consistent with reported CH_4 hyperfine splittings.[24] Extrapolation of this observed time dependence to zero time leads us to conclude that hyperfine depolarization effects are negligible for the Δ_p measurements performed at an excitation distance of 1 mm from the surface (0.35–1 μsec excitation-to-surface delay for the molecular beam velocities used in the presented experiments).
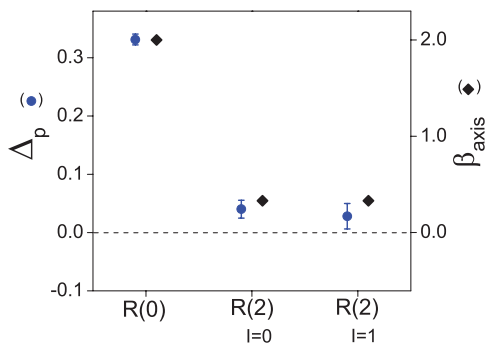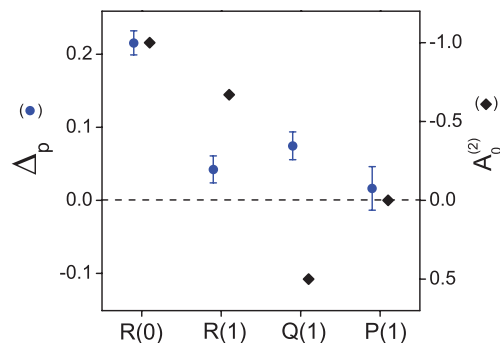
FIG. 6. Comparison of the alignment contrast for $CH_4(\nu_3)$ on Ni(110) for excitation via R(0) and R(2) at a distance of 1 mm from the surface. The R(2) line consists of two separate components due the ortho (I = 1) and para (I = 0) nuclear spin isomers of CH_4. The similar Δ_p values observed for both R(2) components confirms that hyperfine depolarization is insignificant for excitation at 1 mm from the surface.
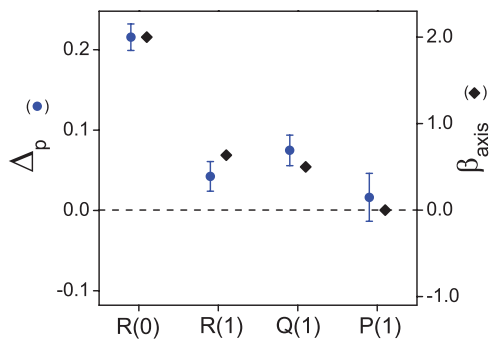
A second test of dephasing effects was performed by preparing $CH_4(\nu_3)$ via the R(2) rovibrational transition which is split due to centrifugal interaction into E and F_2 symmetry components. The transition R(2)-E at 3048.1532 cm^{-1} and R(2)-F_2 at 3048.1690 cm^{-1} excite ortho-(I = 1) and para-(I = 0) CH_4, respectively.[26] The two components of the R(2) transitions are separated by 475 MHz, and are partially overlapped in the room temperature cell spectrum (see Fig. 1) due to Doppler broadening (FWHM ~280 MHz). However, due to the very narrow absorption linewidths of only a few MHz in the molecular beam, we can selectively excite either component of the R(2) transition. Comparison of the Δ_p values measured separately for the I = 1 and I = 0 component of the $CH_4(\nu_3)$-R(2) transition for excitation 1 mm from the Ni(110) surface, probes the extent of hyperfine depolarization during the 500 nsec flight time between excitation and surface dissociation since this dephasing mechanism is absent for para-$CH_4(\nu_3)$ with zero total nuclear spin (I = 0). If the Δ_p value measured for preparation via the I = 0 component of R(2) were significantly larger than Δ_p for the (I = 1) R(2) transition, it would indicate a dephasing of the prepared alignment due to a coupling between $\vec{J}$ with $\vec{I}$ in the latter case. We can exclude such an effect since Δ_p measured for two nuclear spin isomers of $CH_4(\nu_3)$-R(2) are identical within their error bars (Fig. 6). Potentially, magnetic field depolarization might play a role very close to the ferromagnetic Ni crystal. The fact that Δ_p measured for the CH_4 dissociation on diamagnetic Pt(111) is similar to the values observed on Ni single crystals (not shown) allows us to exclude the latter effect.

RESULTS

Using the methods described above, we performed state-resolved reactivity measurements for $CH_4(\nu_3)$ dissociation on Ni(100), Ni(110), and Ni(111). For Ni(100) and Ni(110), we determined the alignment contrast Δ_p for excitation via different rovibrational transitions. Comparison of the experimentally observed alignment contrast Δ_p with the calculated rotational alignment coefficients $A_0^{(2)}$ and vibrational alignment coefficients β_{axis} for P, Q, and R-branch transitions provides information about which of the two quantities

(a)

(b)

FIG. 7. Comparison of the experimentally determined Δ_p values for $CH_4(\nu_3)$ to (a) the corresponding calculated $\vec{J}$ alignment coefficients $A_0^{(2)}$. (b) the corresponding calculated vibrational alignment coefficients β_{axis}. Error bars represent $\pm 2\sigma$ of the average of 4–9 replicate measurements.

control the observed alignment dependence of the methane reactivity.[22,27–29]

Figure 7 shows a comparison of the experimentally observed alignment contrast Δ_p on Ni(100) with the calculated alignment coefficients $A_0^{(2)}$ and β_{axis}, respectively, for $CH_4(\nu_3)$ prepared via the indicated transition (E_{TRANS} = 34 kJ/mol). The vertical axes are scaled such that the origins and the values associated with R(0) excitation coincide for Δ_p and the corresponding calculated alignment coefficient. The change in sign of the calculated $A_0^{(2)}$ alignment coefficients in switching from R-branch to Q-branch excitation (Fig. 7(a)) is not observed in the data for Δ_p.

Contrary to the sign change for $A_0^{(2)}$, the β_{axis} alignment coefficients are positive for both R- and Q-branch excitation, which signifies an alignment of the C–H stretch parallel to the polarization axis in both cases. Inspection of the calculated alignment coefficients β_{axis} in Figure 7(b) shows a much better match with the observed variations in the Δ_p values both in sign and magnitude than with the calculated $A_0^{(2)}$ coefficients, indicating that the C–H stretch alignment is primarily responsible for the observed steric effects in methane reactivity.[22]

ANGLE DEPENDENCE OF THE ALIGNMENT EFFECT ON Ni(100)

In addition to the reactivity measurements with laser polarization parallel and normal to the surface, we explored the
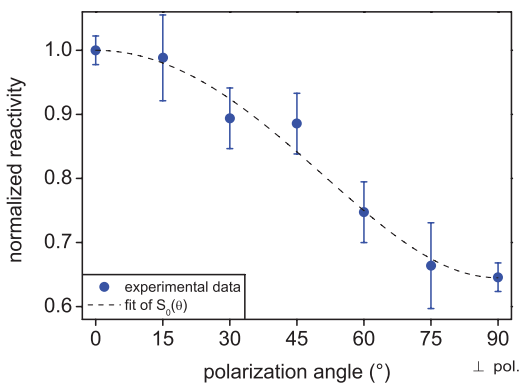
FIG. 8. Polarization angle dependence of the alignment effect on Ni(100) for CH$_4(\nu_3)$ prepared via R(0) excitation (E$_{TRANS}$ = 34 kJ/mol).

polarization angle (θ) dependence of the reactivity of CH$_4(\nu_3$ = 1, J = 1) excited via R(0) on Ni(100) in 15° steps from parallel to normal. The observed reactivity decreases monotonically from a maximum for in-plane laser polarization (II-pol.) to a minimum when the polarization direction is along the surface normal (Fig. 8). The angle dependence S$_0(\theta)$ between 0 and 90° can be described by a simple expression using a geometric decomposition into S$_0^{\parallel}$ and S$_0^{\perp}$, where S$_0^{\perp}$ = 0.65 × S$_0^{\parallel}$

$$S_0(\theta) = \sqrt{\left(S_0^{\parallel}\right)^2 - \sin^2\theta\left[\left(S_0^{\parallel}\right)^2 - \left(S_0^{\perp}\right)^2\right]}. \quad (4)$$

ALIGNMENT EFFECTS ON Ni(110)

For the anisotropically corrugated Ni(110) surface, we measured both the polar and the azimuthal polarization angle dependence of the methane reactivity (see Fig. 9). The Ni(110) surface consists of rows of closely packed Ni atoms located in the topmost layer which are separated by one layer deep troughs. The (110) surface is generated by a cut across the diagonal of the face-centered cubic lattice. This cut produces a spacing between rows of 3.52 Å, while the close-packed Ni atom spacing in each row is 2.49 Å.[30,31] The fact that the nickel surface sample is a single crystal makes it possible to align the direction of the rows and troughs in the laboratory frame simply by rotating the 10 mm diameter disk. We aligned the Ni(110) surface rows in the laboratory frame to within 3.2° of true vertical and 1.7º of horizontal in order to achieve the – *parallel* ($\varphi = 0°$) and – *perpendicular* ($\varphi = 90°$) configurations shown in Figure 9. The highest reactivity was observed for in-plane alignment of the polarization of the excitation laser perpendicular to the close-packed rows of Ni atoms (*perpendicular* configuration). Rotating the laser polarization in the surface plane by 90° to be parallel to the close-packed rows reduces the reactivity by approximately 30%. A further 90° rotation of the laser polarization out of the surface plane along the surface normal causes the reactivity to drop further by 44%. Combining the two rotations, the reactivity of CH$_4(\nu_3)$ on Ni(110) at E$_{TRANS}$ = 34 kJ/mol increases by a factor of 2.5 from the least reactive S$_0^{\perp}$ to the most reactive S$_0^{\parallel}(\varphi = 90°)$ alignment (see Fig. 10).
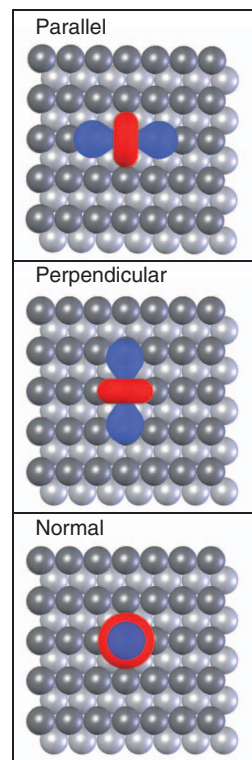

FIG. 9. Schematic of the state-prepared and laser aligned molecular beam deposition experiment on Ni(110). Probability distributions for $\vec{J}$ (red) and $\vec{\mu}_{if}$ (blue) are shown for ν_3-excitation via the R(0) transition by linearly polarized radiation. (Top) Polarization axis in the plane of the surface and parallel to the close-packed rows of Ni atoms: "*parallel*" configuration. (Middle) Polarization axis in the plane of the surface and perpendicular to the close-packed rows of Ni atoms: "*perpendicular*" configuration. (Bottom) Polarization axis normal to the plane of the surface: "*normal*" configuration.

Analogous to the data shown in Figure 7 for Ni(100), we measured the alignment dependent dissociation of CH$_4(\nu_3)$ on Ni(110) for excitation via the three rotational branches. In Figure 11, we compare $\Delta_p(\varphi = 90°)$ to calculated alignment coefficients for CH$_4(\nu_3)$ prepared by three rovibrational transitions: R(0), Q(1), and P(1). As was the case on Ni(100), values of $\Delta_p(\varphi = 90°)$ are positive for both R- and Q-branch excitation and scale with the vibrational alignment coefficient β_{axis}.
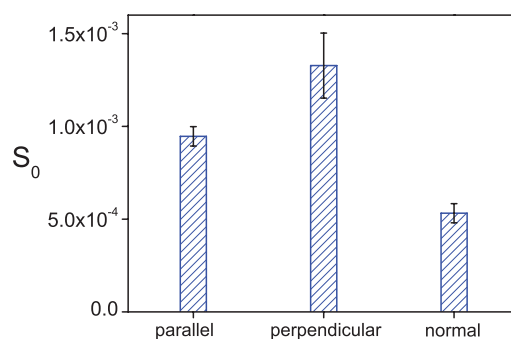

FIG. 10. Initial reaction probability (S$_0$) for 34 kJ/mol translational energy CH$_4(\nu_3)$-R(0) in the *parallel*, *perpendicular*, and *normal* configuration dissociating on Ni(110). Error bars are ±2σ of the mean from replicate measurements.
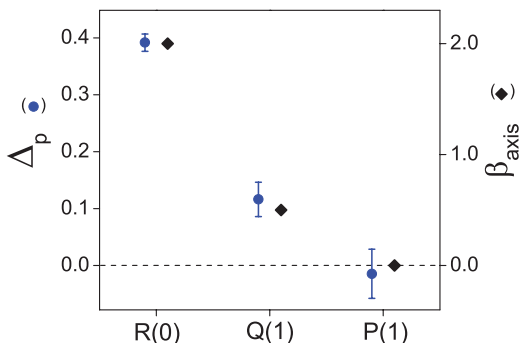
FIG. 11. Comparison of alignment contrast Δ_p for $CH_4(\nu_3)$ prepared via R(0), P(1), Q(1) transitions on Ni(110) – perpendicular configuration with the corresponding β_{axis} coefficients. The vertical axes are scaled such that their origins and the values for the R(0) excitation coincide. $E_{TRANS} = 34$ kJ/mol. Error bars represent $\pm 2\sigma$ from replicate measurements.

FIG. 13. Initial reaction probability of methane as a function of translational energy on Ni(110). Error bars represent $\pm 95\%$ confidence from student-T statistics on replicate measurements.

ALIGNMENT EFFECTS ON Ni(100), Ni(110), AND Ni(111) AS A FUNCTION OF INCIDENT TRANSLATIONAL ENERGY

Figure 12 shows a comparison of the alignment contrast Δ_p for $CH_4(\nu_3)$-R(0) excitation on Ni(111), Ni(100), and Ni(110) at $E_{TRANS} = 34$ kJ/mol together with the variation of Δ_p with incident translational energy for Ni(100) and Ni(110). Two values, $\Delta_p(\varphi = 0°)$ and $\Delta_p(\varphi = 90°)$ are shown for Ni(110) at $E_{TRANS} = 34$ kJ/mol. The magnitude of the alignment effect decreases from Ni(110) to Ni(100) and Ni(111). There is no discernible translational energy dependence of Δ_p for Ni(100) and Ni(110) in the range of 9–65 kJ/mol which indicates that steering effects, which could reorient the incident molecules along their minimum energy pathway to reaction, are too weak to produce an observable effect on the sub-picosecond timescale probed in this incident energy range.

DISCUSSION

Our stereodynamics study of the reactivity of $CH_4(\nu_3)$ on Ni(100), Ni(110), and Ni(111) yielded several results that may help to explain the steric effects in the chemisorption of vibrationally excited methane reported recently for the first time.[15] First, both on Ni(100) and Ni(110), we find the align-
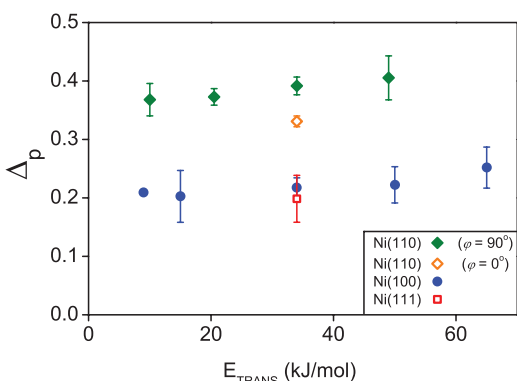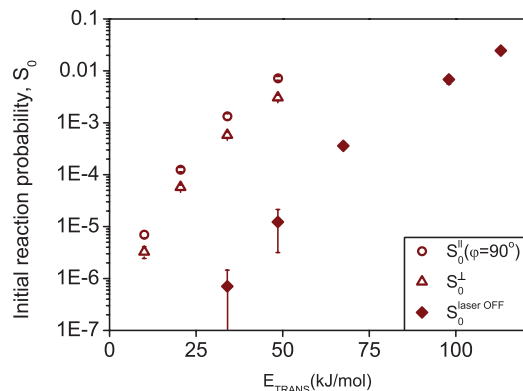

FIG. 12. Comparison of alignment contrast Δ_p for $CH_4(\nu_3)$-R(0) excitation on Ni(111), Ni(100), and [*parallel* ($\varphi = 0°$) and *perpendicular* ($\varphi = 90°$)] on Ni(110) as a function of translational energy (E_{TRANS}) of the molecular beam. Error bars represent $\pm 2\sigma$ from replicate measurements.

ment dependence of the $CH_4(\nu_3)$ reaction probability to be correlated with an alignment of the C–H stretch with respect to the surface. C–H stretch alignment in the plane of the surface makes methane more reactive than alignment along the surface normal. Second, the alignment effect is significantly larger on Ni(110) than on Ni(100) and Ni(111). Third, on the anisotropically corrugated Ni(110) surface, aligning the C–H stretch in the surface plane and perpendicular to the close-packed rows of Ni(110) results in a larger alignment contrast Δ_p than aligning it parallel to the close-packed rows. Finally, the alignment dependence of the $CH_4(\nu_3)$ reactivity on Ni(110) and Ni(100) is found to be independent of incident translational energy between at least 10 and 50 kJ/mol, even though the absolute reaction probability of $CH_4(\nu_3)$ on Ni(110) increases by three orders of magnitude over the same translational energy range (see Fig. 13).

The fact that Δ_p scales with β_{axis} (Fig. 7 and 11) indicates that the alignment dependence of the methane reactivity is primarily due to an alignment of the C–H stretch and not the angular momentum J. Simpson *et al.*[22] arrived at an analogous conclusion in their stereodynamics study of the gas phase reaction of $CH_4(\nu_3)$ and $CD_3H(\nu_1)$ with chlorine atoms. As discussed in Simpson *et al.*,[22] R(0) excitation of the triply degenerate ν_3 vibration prepares CH_4 in a state with J = 1, l = 1, and N = 0 where J, l, and N are the quantum numbers for total, vibrational, and rotational angular momentum, respectively. In this state, CH_4 possesses one quantum of vibrational angular momentum and no rotational angular momentum, resulting in a rotationless molecule with a spatially isotropic rotational wavefunction (s-orbital). Therefore, only the net C–H stretch amplitude is polarized in the laboratory frame by the laser excitation while the orientation of its four C–H bonds remains unspecified. Since we observe the strongest alignment effect for R(0) excitation, this indicates that the alignment effect cannot be due to an alignment of any of the four C–H bonds relative to the plane of the surface but is rather due to an alignment of the net C–H stretch amplitude. The CH_4 reactivity is observed to decrease continuously with increasing angle θ between the laser polarization and the plane of the surface from parallel ($\theta = 0$) to normal ($\theta = 90°$) (Fig. 8).

The underlying mechanism for the observed alignment effects is not immediately obvious. Before we can interpret

the observations as a steric effect of the ν_3-excited methane reactivity, we need to consider the possibility that the rate of vibrational energy transfer from the incident methane molecule to the metal surface depends on the C–H stretch alignment. Classically, the vibrationally excited molecule can be represented as an oscillating electric dipole, which induces an image dipole in the conducting surface. The interaction of an oscillating electric dipole with its image dipole is alignment dependent and is related to the surface dipole selection rule of reflection absorption infrared spectroscopy of adsorbates on a metal surface.[32] Classical electrodynamics predicts a friction force acting on a moving charge in front of a conducting surface with a normal component that is twice larger than the parallel component.[33,34] Therefore, the frictional damping of an oscillating electric dipole will be stronger for normal than for parallel alignment, in qualitative agreement with the alignment effect reported here. The measured higher reactivity for $CH_4(\nu_3)$ with the C–H stretch amplitude aligned parallel to the surface plane could be due to a larger fraction of incident molecules remaining in their vibrationally excited state because of the smaller frictional damping force for parallel alignment as compared to normal alignment. However, this classical image dipole model becomes invalid at very small distances of the dipole from the surface and has to be replaced by a quantum mechanical treatment including electronically nonadiabatic effects such as the independent surface hopping model developed by Tully and co-workers for the description of the scattering of highly vibrationally excited NO from Au(111) surface.[35,36]

For the alignment dependent friction argument to be applicable, the rate of vibrational energy transfer between the incident methane molecules and the nickel surface needs to be fast enough for significant vibrational energy transfer to occur on the sub-picosecond timescale of the hyperthermal methane/surface collisions in our experiments. Vibrational lifetimes of strongly bound, chemisorbed species such as CO and CN on transition metals have been measured to be on the order of a few psec by time resolved pump-probe techniques[37–39] and lifetimes of physisorbed species can be expected to be significantly longer. Luntz and co-workers did consider the possibility of nonadiabatic effects in adsorption, desorption, and scattering of H_2 (D_2) on Cu and N_2 on Ru.[40,41] They found that electronic friction increased along the reaction path toward the transition state to a value significantly larger than molecularly adsorbed state. However, little is known about the rate of vibrational relaxation via electron-hole pair excitation during hyperthermal collisions of the vibrationally excited methane with a surface. Even at the highest incident energy studied here, reactive collisions of the incident $CH_4(\nu_3)$ remain the minority channel ($<1\%$). It is still an open question what fraction of the $>99\%$ unreactive $CH_4(\nu_3)$/Ni collisions are vibrationally inelastic where the scattered CH_4 has either lost at least part of its vibrational energy to surface degrees of freedom or has undergone intramolecular vibrational redistribution (IVR) during the collision with the metal surface. Detection techniques to probe the vibrational state distribution of the scattered CH_4 are in preparation in our laboratory to shed light on this important question.

Even in the absence of vibrational energy transfer between the incident methane molecule and the metal surface, short range molecules/surface interactions can lead to surface-induced IVR, a process which could be alignment dependent. In this process, the incident methane molecules, which were initially prepared by single-mode laser excitation in a stationary rovibrational eigenstate, experience time-dependent intermolecular vibrational energy flow due to their interaction with the metal surface. Such surface induced IVR has been included in the four-dimensional vibrationally adiabatic model calculations of Halonen *et al.*[9] to predict the possibility of mode-specific reactivity of CH_4. Halonen's model suggests that intramolecular vibrational energy flow within the reactant molecule during its approach to the metal surface depends on the initially prepared eigenstate and that different energy localization can lead to different reactivity even though the total internal energy are nearly identical. In recent work, Nave and Jackson[11] have developed a first-principles full fifteen-dimensional reaction path Hamiltonian treatment of the reaction of CH_4 on Ni(100) which includes surface induced IVR as well as vibrationally non-adiabatic transitions and which permits the computation of state-resolved reaction probabilities. Their calculations confirm the mode-specific CH_4 reactivity predicted by Halonen *et al.*[9] in agreement with experimental measurements of state-resolved CH_4 reactivity.[42] If surface-induced IVR does not only depend on the initially prepared rovibrational quantum state but also on alignment of the C–H stretch amplitude relative to the surface plane it may be responsible for the observed steric effects. This alignment dependent IVR mechanism implies the absence of significant steering forces, which could reorient (realign) the incident vibrationally excited molecule into its lowest energy configuration during the approach to the surface consistent with our observation that there is no discernible dependence of the alignment effect on incident translational energy.

Finally, if steering is either weak or absent, the observed alignment dependence may simply be a consequence of the complex multidimensional potential energy hypersurface. Different initial vibrational alignments of the incident molecules may follow different reactive trajectories sampling a barrier height that is dependent on the alignment coordinate.

To conclude, our data demonstrates that methane dissociation on a nickel surface is a complex process, which depends on many parameters of the molecule/surface encounter. For a more detailed and quantitative interpretation of the observed alignment effects on different orientations of the Ni surface, comparison should be made with results of multi-dimensional quantum dynamics calculations, including the alignment coordinates. Such calculations are currently being pursued in at least two theory groups.[11,13] Our detailed, state-resolved reactivity data should be helpful in the development of a predictive theoretical understanding of this important gas/surface reaction.

[1]C. T. Rettner, H. E. Pfnur, and D. J. Auerbach, Phys. Rev. Lett. **54**, 2716 (1985).

[2]C. T. Rettner, H. E. Pfnur, and D. J. Auerbach, J. Chem. Phys. **84**, 4163 (1986).

[3]R. D. Beck, P. Maroni, D. C. Papageorgopoulos, T. T. Dang, M. P. Schmid, and T. R. Rizzo, Science **302**, 98 (2003).

[4]D. R. Killelea, V. L. Campbell, N. S. Shuman, and A. L. Utz, Science **319**, 790 (2008).

[5]L. B. F. Juurlink, D. R. Killelea, and A. L. Utz, Prog. Surf. Sci. **84**, 69 (2009).

[6]J. Harris, J. Simon, A. C. Luntz, C. B. Mullins, and C. T. Rettner, Phys. Rev. Lett. **67**, 652 (1991).

[7]A. P. J. Jansen and H. Burghgraef, Surf. Sci. **344**, 149 (1995).

[8]M. N. Carre and B. Jackson, J. Chem. Phys. **108**, 3722 (1998).

[9]L. Halonen, S. L. Bernasek, and D. J. Nesbitt, J. Chem. Phys. **115**, 5611 (2001).

[10]R. Bisson, M. Sacchi, and R. D. Beck, Phys. Rev. B **82**, 121404 (2010).

[11]S. Nave and B. Jackson, Phys. Rev. B **81**, 233408 (2010).

[12]K. G. Prasanna, R. A. Olsen, A. Valdes, and G. J. Kroes, Phys. Chem. Chem. Phys. **12**, 7654 (2010).

[13]G. P. Krishnamohan, R. A. Olsen, G. J. Kroes, F. Gatti, and S. Woittequand, J. Chem. Phys. **133**, 144308 (2010).

[14]B. Jackson and S. Nave, J. Chem. Phys. **135**, (2011).

[15]B. L. Yoder, R. Bisson, and R. D. Beck, Science **329**, 553 (2010).

[16]M. P. Schmid, P. Maroni, R. D. Beck, and T. R. Rizzo, Rev. Sci. Instrum. **74**, 4110 (2003).

[17]R. N. Zare, Ber. Bunsenges. Phys. Chem. **86**, 422 (1982).

[18]W. R. Simpson, A. J. Orrewing, T. P. Rakitzis, S. A. Kandel, and R. N. Zare, J. Chem. Phys. **103**, 7299 (1995).

[19]W. Demtröder, *Laser Spectroscopy: Basic Concepts and Instrumentation* (Springer-Verlag, Berlin, 1998).

[20]N. V. Vitanov, T. Halfmann, B. W. Shore, and K. Bergmann, Annu. Rev. Phys. Chem. **52**, 763 (2001).

[21]R. N. Zare, *Angular Momentum: Understanding Spatial Aspects in Chemistry and Physics* (Wiley, New York, 1988).

[22]W. R. Simpson, T. P. Rakitzis, S. A. Kandel, A. J. Orr-Ewing, and R. N. Zare, J. Chem. Phys. **103**, 7313 (1995).

[23]E. H. Van Kleef and I. Powis, Mol. Phys. **96**, 757 (1999).

[24]J. L. Hall and C. Borde, Phys. Rev. Lett. **30**, 1101 (1973).

[25]J. McHale, *Molecular Spectroscopy* (Prentice-Hall, London, 1999).

[26]L. S. Rothman, I. E. Gordon, A. Barbe, D. C. Benner, P. E. Bernath, M. Birk, V. Boudon, L. R. Brown, A. Campargue, J.-P. Champion, K. Chance, L. H. Coudert, V. Dana, V. M. Devi, S. Fally, J.-M. Flaud, R. R. Gamache, A. Goldman, D. Jacquemart, I. Kleiner, N. Lacome, W. J. Lafferty, J.-Y. Mandin, S. T. Massie, S. N. Mikhailenko, C. E. Miller, N. Moazzen-Ahmadi, O. V. Naumenko, A. V. Nikitin, J. Orphal, V. I. Perevalov, A. Perrin, A. Predoi-Cross, C. P. Rinsland, M. Rotger, M. Simeckova, M. A. H. Smith, K. Sung, S. A. Tashkun, J. Tennyson, R. A. Toth, A. C. Vandaele, and J. Vander Auwera, J. Quant. Spectrosc. Radiat. Transf. **110**, 533 (2009).

[27]W. R. Simpson, T. P. Rakitzis, S. A. Kandel, T. Levon, and R. N. Zare, J. Phys. Chem. **100**, 7938 (1996).

[28]A. J. OrrEwing, W. R. Simpson, T. P. Rakitzis, S. A. Kandel, and R. N. Zare, J. Chem. Phys. **106**, 5961 (1997).

[29]J. P. Camden, H. A. Bechtel, D. J. A. Brown, and R. N. Zare, J. Chem. Phys. **124**, 034311 (2006).

[30]D. F. Mitchell, P. B. Sewell, and M. Cohen, Surf. Sci. **69**, 310 (1977).

[31]N. D. M. Neil and W. Ashcroft, *Solid State Physics* (Saunders, Fort Worth, 1976).

[32]M. Trenary, Annu. Rev. Phys. Chem. **51**, 381 (2000).

[33]B. N. J. Persson and W. L. Schaich, J. Phys. C: Solid State Phys. **14**, 5583 (1981).

[34]B. N. J. Persson and S. Andersson, Phys. Rev. B **29**, 4382 (1984).

[35]S. Roy, N. A. Shenvi, and J. C. Tully, J. Chem. Phys. **130**, 174716 (2009).

[36]N. Shenvi, S. Roy, and J. C. Tully, Science **326**, 829 (2009).

[37]M. E. Schmidt and P. Guyot-Sionnest, J. Chem. Phys. **104**, 2438 (1996).

[38]C. Matranga and P. Guyot-Sionnest, Chem. Phys. Lett. **340**, 39 (2001).

[39]M. Morin, N. J. Levinos, and A. L. Harris, J. Chem. Phys. **96**, 3950 (1992).

[40]A. C. Luntz and M. Persson, J. Chem. Phys. **123**, 074704 (2005).

[41]A. C. Luntz, M. Persson, and G. O. Sitz, J. Chem. Phys. **124**, 091101 (2006).

[42]P. Maroni, D. C. Papageorgopoulos, M. Sacchi, T. T. Dang, R. D. Beck, and T. R. Rizzo, Phys. Rev. Lett. **94**, 4 (2005).